UNCONVENTIONAL RESOURCES TECHNOLOGY CONFERENCE
FUELED BY SPE • AAPG • SEG

URTeC: 4043632

Avoiding the Salts: Strategic Fracture Propagation Management for Enhanced Stimulation Efficiency in the Cane Creek Play

No'am Zach Dvory*[1], John David McLennan[2], Ankush Singh[3], Brian James McPherson[1], 1. Civil & Environmental Engineering & Energy and Geoscience Institute, The University of Utah, USA, 2. Chemical Engineering & Energy and Geoscience Institute, The University of Utah, 3. ResFrac Corporation.

Abstract

This study analyzes hydraulic fracturing strategies in the Cane Creek Play of the Pennsylvanian-age Paradox Formation. This is a challenging yet prospective unconventional tight oil play in southeastern Utah. Recognizing the geomechanical complexities of the region, along with the opportunities, there is a need to develop sustainable and economic stimulation techniques to optimize hydraulic fracture propagation within the play. A key challenge identified in the Cane Creek Play involves controlling fracture propagation to prevent extension into adjacent thick salt formations, which leads to operational difficulties and reduced production efficiency. The study focuses on assessing the roles of fracture toughness and stress variation in influencing fracture development. Integrating fracture toughness measurements from various literature sources and discrete measurements within the Cane Creek play and salt deposits provides an understanding of the fracture toughness profile, essential for fracture geometry design. The study also uses advanced simulation tools to explore the impact of varying cluster spacing and fluid volumes on fracture propagation. In this geologic setting, the findings indicate, as expected, that tighter cluster spacing and reduced fluid volumes effectively limit fracture propagation within the productive zones. Stress shadowing and proppant transport are also relevant in fracture development in this field. Potential refinements include modifying cluster spacing and fluid volumes based on the specific geological characteristics, managing stress shadow effects, and continuously employing simulation tools for improved understanding and design of fracturing operations.

Introduction

The Cane Creek Play in the Pennsylvanian-age Paradox Formation in southeastern Utah is regarded as a promising yet challenging unconventional tight oil play in the US, with a history of drilling difficulties and spotty stimulation success. Initially identified nearly a century ago, substantial exploration resumed only in the early 1990s with the advent of horizontal drilling technology. Despite some successful wells, achieving substantial production remained elusive. This project aims to leverage knowledge of the basin's geomechanical attributes and suggest sustainable and economic stimulation strategies.

Hydraulic fracture design exercises are important in this setting since the stimulation targets are thin and hydraulic fractures that run into the thick, proximal (adjacent) salt formations cause a backflow of brines that plug the well and increase the operational costs. Here we will consider the effect of the stress layering and the fracture toughness, which are relevant parameters for site characterization and fracture geometry forecasting. The local orientation and magnitude of the in-situ stresses dictate the direction in which fractures will propagate. Understanding the stress profiles ensures that fractures grow in the desired direction, optimizing the connection to the reservoir. Moreover, as is well known, identifying stress barriers formed by layers with higher stress relative to adjacent layers demarcates the containment of hydraulic fractures. This may mitigate unwanted fluid migration or avoid fracturing non-target zones, which can lead to decreased production or environmental issues. Other direct fracture management aspects related to stress layering are optimizing proppant placement, fault reactivation management, and designing the fracturing fluids. Designing fracturing fluid properties under a known stress field can assist, through viscosity management, in limiting the fractures' migration into the salts. This could have a particular value in the Paradox evaporite sequences.

Hydraulic fracture propagation is influenced by fracture toughness and the resistance to fluid flow (Dontsov and Suarez-Rivera, 2020). Those authors show that in a viscosity-dominated regime, fractures demonstrate minimal stress shadow interactions, expanding predominantly in a radial fashion and exhibiting quasi-isotropic geometry. Conversely, in a toughness-dominated regime, fractures experience more pronounced stress shadow interactions—some growing as individual segments while others propagating simultaneously. This behavior culminates in geometric structures reminiscent of flower petals, where the overall geometry maintains a radial uniformity, yet individual fractures form non-overlapping segments of the total surface area. To simulate fracture propagation and formulate protocols for constraining fracture dimensions under such conditions, we adopted the "planar fracture modeling" approach (McClure et al., 2020). This numeric modeling approach amalgamates hydraulic fracturing, wellbore overprints, and reservoir dynamics and addresses fluid components, including water, oil, gas, slurry modifiers, and additives such as high-viscosity friction reducers and specified proppant types (McClure and Kang, 2018). Solving mechanical equilibrium equations determines stress variations from crack expansion and matrix fluid pressure alteration. These calculations ensure that all governing equations are satisfied across every element and timestep. Hydraulic fractures are represented by meshed cracks with apertures ranging from microns to millimeters. Proppant transport includes gravitational settling, bed slumping, and proppant trapping. Additionally, flow equations account for relative permeability, gravitational impacts, non-Darcy pressure variances, and non-Newtonian fluid behavior. In addition, the perforation pressure drop for each cluster is ascertained by considering factors like shot number, diameter, and discharge coefficient using accepted methods.

For the Paradox basin application, we used stimulation data from the recently drilled horizontal well in State 16-2 LN to analyze the fracture profile sensitivity and evaluate how varying cluster spacing influences fracture length. We did not consider the implications of manipulating fluid viscosity. While different

viscosity fluids might limit fracture propagation into the salts, they were not considered in this study's framework.

The Paradox Oil Play - a multistage hydraulic stimulation field test

The US Department of Energy, through the National Energy Technology Laboratory, has funded the University of Utah and Zephyr Energy to undertake data acquisition and interpretation during the drilling and development of one vertical well and two horizontal wells at the Northern Paradox basin. The aim has been to identify cost-effective strategies for drilling, completing, and stimulating wells in the structurally intricate Pennsylvanian Cane Creek shale and surrounding clastic zones. Previously, natural fractures/faults have been identified as playing an important role in several offset production wells. The success rate of stimulations relying on accessing natural fractures isn't consistent. It's hypothesized that improving production in this play could partially depend on a refined characterization of the stress state. Additional requirements are comprehensive characterization, quantification, and analysis of the geological, structural, and geomechanical features. This analysis aims to highlight factors that could enhance production.

The project includes one pilot vertical well (State 16-2) and one horizontal well (State 16-2 LN) (Figure 1). Another well (State 36-2) experienced a well control incident during April 2023 and is expected to be redrilled. Approximately 110 feet of core and well logs, including a Formation Microimager, were gathered from the State 16-2 vertical pilot hole and the State 16-2 LN. A detailed assessment of the natural fracture distribution in the core from the State 16-2 vertical well was carried out Cooper and Lorenz (2022). Through this core analysis and fracture description, 100 relevant fractures were described within Cane Creek. Image log analysis in the State 16-2 LN showed 177 relevant fractures within Cane Creek (Dvory et al., 2024).

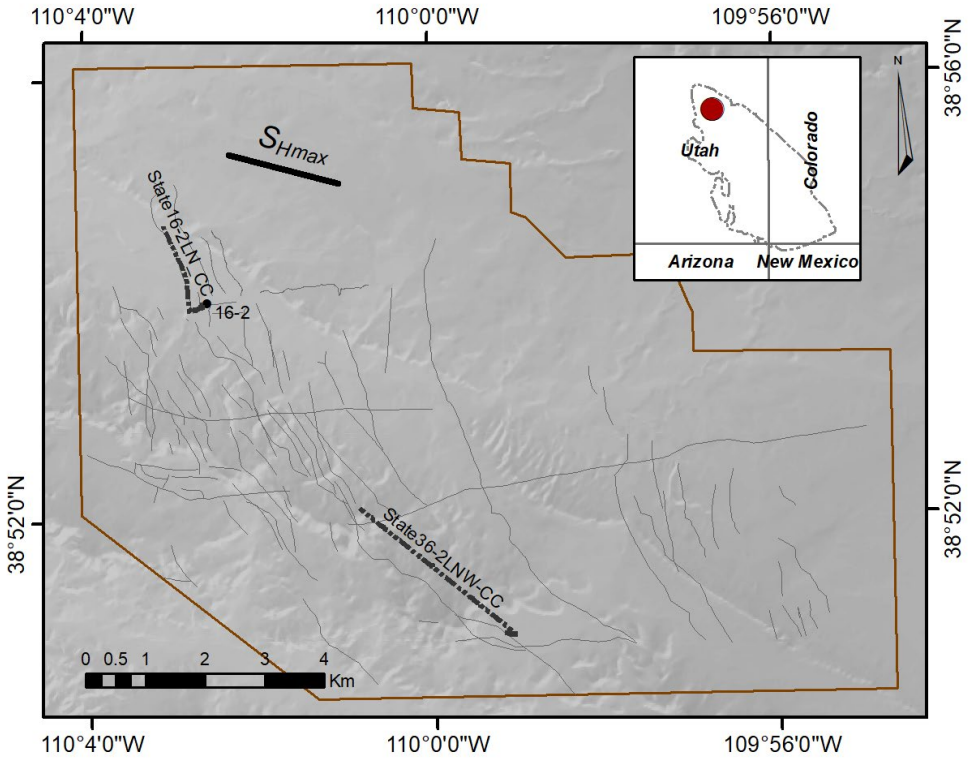

Figure 1. Site location within the Paradox Basin. Gray lines are mapped faults within the Cane Creek Unit.

A diagnostic fracture injection test (DFIT) was performed in State 16-2. The acquired data were analyzed to estimate the minimum horizontal principal stress, $S_{hmin,}$ pore pressure, and matrix permeability. As expected for this locally overpressured play, the DFIT interpretation yielded a significantly elevated pore pressure and S_{hmin}, indicating a stress difference between the overburden and the minimum horizontal stress of a few hundred psi, consistent with the overpressure and the presence of halite.

The State 16-2 LN operation used 5.5-inch, 20-pound per foot P-110 grade tubing, aiming for a bottom depth of 14,370 feet MD. The hydraulic fracturing program had 14 stages with a ~160 ft geometric stage length. Each stage had five perforation clusters spaced at 32 ft. Each perforation cluster had 6 shots for a total of 30 shots per stage, and each perforation was predicted to have had a nominal entry hole diameter of 0.33 in. We considered Stage 11 a representative example of the design fracturing procedure and performance for the current investigation. During Stage 11, 2,418.5 barrels of clean fluid and 2,650.4 barrels of slurry were pumped into the well. A 7.5% hydrochloric acid spearhead in front of slickwater was later followed by 103,580 pounds of 20/40 and 100 mesh Northern White proppant. Operational pressures peaked at 9,290 psi at the surface, with an average maintained at 8,605 psi. The maximum treating rate was 81.4 barrels per minute. Technical metrics, including a fracturing gradient of 1.09 psi/ft.

Fracture Toughness

Fracture toughness is a misunderstood knob on most hydraulic fracturing simulators. Mode I fracture toughness property quantifies a material's resistance to fracture propagation (planar normal tension) or, in other words, its ability to withstand fracture extension. Understanding fracture toughness could be relevant for Cane Creek simulation optimization. The Paradox stratigraphy within the Cane Creek play is repeated sequences of clastic units and salts. This presents a challenge since both the clastic units and the salts have relatively lower fracture toughness and consequently require less energy for the fractures to propagate further away from the well (Meng et al., 2015; Li et al., 2020; Wang et al., 2022). The nominal thickness of the Cane Creek play is 100 ft, and the thickness of the oil-bearing sections is about 10 ft. Consequently, a fracture that propagates a few hundred feet into the upper or lower salt sequences is probably not contributing to the production rate – and is detrimental because of contact with the salt. Moreover, the fracture toughness of the salts is lower than the fracture toughness of the clastic units, which encourages fracture propagation further into the salt. We amalgamated reported fracture toughness values from various literature sources with discrete measurements from the Cane Creek clastic units and the Paradox salt deposits to hypothesize a fracture toughness profile for input into our numerical modeling. Most of the experiments we conducted were on sandy siltstone. Additionally, we tested one sample of salt and one anhydritic dolomudstone (Figure 2, Table 1). A similar parameter range was found in the literature (Meng et al., 2015; Li et al., 2020; Wang et al., 2022). Figure 2 includes a few examples from the literature that showcase the change of fracture toughness that might occur due to temperature, loading rates, and fluid interaction processes. For instance, Wang et al. (2022) investigated the fracture toughness of halite under varying temperatures and loading rates, revealing an increase in fracture toughness with the rise of both temperature and loading rate (Figure 2), as ductility and blunting potential increase. Li et al. (2020) examined the impact of temperature on the stability and compactness of gypsum, demonstrating that within a restricted reservoir temperature range (68°C to 100°C as indicated by mud logs), the fracture surfaces were smooth, exhibiting a trans-granular fracture mode. They also highlighted a weakening of the gypsum due to thermal dehydration, which converts calcium sulfate dihydrate to β-calcium sulfate and γ-calcium sulfate. Meng et al. (2015) analyzed the fracture toughness of interlayered gypsum associated with a bedded salt deposit under different fluids and temperatures. They correlated porosity change rates with different fluids to fracture toughness trends.

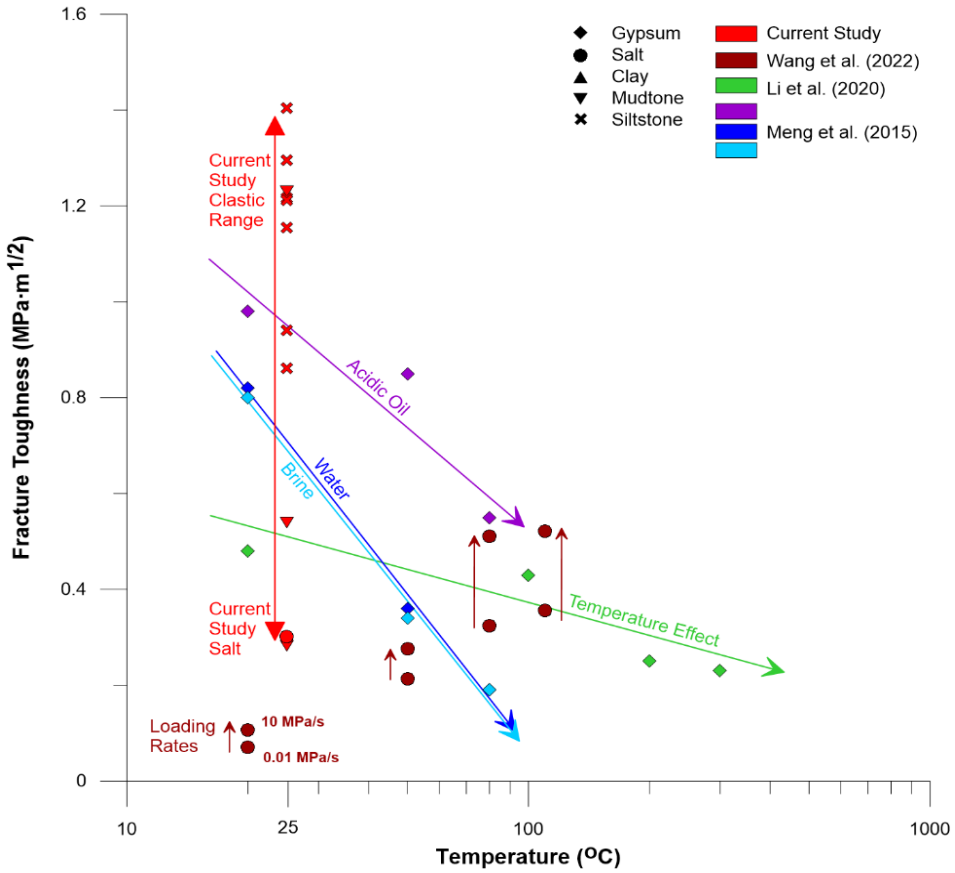

Figure 2. Dynamics of fracture toughness due to changes in temperature, loading rates, and fluid interaction processes. Data from the current study investigation, Meng et al. (2015), Li et al. (2020) and Wang et al. (2022). The downhole temperature in well 16-2 was 71^{O}C. (the logarithmic scale is utilized for easier visualization).

Table 1. Laboratory K_{IC} (Mode I fracture toughness) measurements on core from well State 16-2.

Measured Depth (ft)	Lithology	Fracture Toughness (MPa·m$^{1/2}$)
9654.3	Anhydritic-dolomudstone	0.28
9658.25	Organic-rich mudstone	1.23
9673.65	Fine grained sandy siltstone	1.40
9680.65	Calcareous silty mudstone	1.15
9689.55	Fine grained sandy siltstone	0.86
9705.55[1]	Fine grained sandy siltstone	1.26
9710.5	Fine grained sandy siltstone	0.94
9716.5	Fine grained sandy siltstone	1.21
9720.5[2]	Organic-rich mudstone	0.54
9745.9	Salt	0.30

1. Two samples average; 2. The only sample to break in three pieces

Stress Layering assessment, also known as Stress "Roughness" through stimulation Initial Shut-In Pressure (ISIP) measurements

Different stresses in different layers impact hydraulic fracture growth (Simonson, 1978; Fu et al., 2019; Singh et al., 2020). Knowledge of the minimum total horizontal stress is required for optimizing stimulations in the context of stage length, perforation cluster spacing, injection volumes, lateral well

spacing, etc. The stress data from well State 16-2 LN, derived from fourteen Initial Shut-In Pressures (ISIPs) gathered during well stimulation, indicates that the lowest principal stress changes depending on the depth and type of rock encountered. Figure 3 shows the trajectory of well State 16-2 LN within the Cane Creek play and the ISIPs for each stimulation stage (red dots). Figure 3 illustrates the designed trajectory of the wellbore, directional changes, and the final landing within the target horizon of the Cane Creek unit. The Cane Creek unit is composed of three zones (Jagniecki et al., 2019). The A Zone in the Cane Creek unit consists of a mix of dolomitic mudstone, calcareous materials, anhydrite, and siltstone, with notable fractures filled with anhydrite and halite. Source rock analysis indicates high organic content and hydrocarbon potential, with maturity data suggesting the presence of both Type I and II kerogen, pointing towards significant hydrocarbon accumulation within the oil window; The B zone of Cane Creek is characterized by bioturbated siltstone-sandstone with a notable porosity of 17%. It contains less anhydrite than other zones, with features including organic-rich mudstone and calcareous mudstone. Mineral analysis shows significant feldspar and mica, suggesting potential micro- to nano-scale porosity. Vertical fractures filled with anhydrite, halite, or calcite, some with bitumen, enhance the zone's reservoir quality. The lower section of this zone is characterized by high porosity and likely good permeability marked in the figure as 'Target B'. The C zone of Cane Creek combines reservoir and source rock elements, marked by dolomitic mudstone, anhydrite, a thick sandstone layer, and organic-rich mudstone. The zone's sandstone,'Target C', is arkosic, less bioturbated than in the B zone, with porosity between 7 to 10% and permeability at 0.197 mD. Organic-rich mudstones, indicating reducing conditions, complement the reservoir's source potential, with a notable TOC of 7.9% and maturity at 0.79 %Vro. The siltstone-sandstone's high porosity and likely good permeability make it a key focus for further analysis and exploration within the Cane Creek formation.

The fourteen ISIP measurements were correlated with seven stratigraphic units within the Cane Creek sequence. Figure 4 shows that the highest S_{hmin} value is in the lower section of the so-called B Zone that exhibits a stress burrier. Fracs that propagate upward will face a smaller stress barrier in the upper section of the same unit.

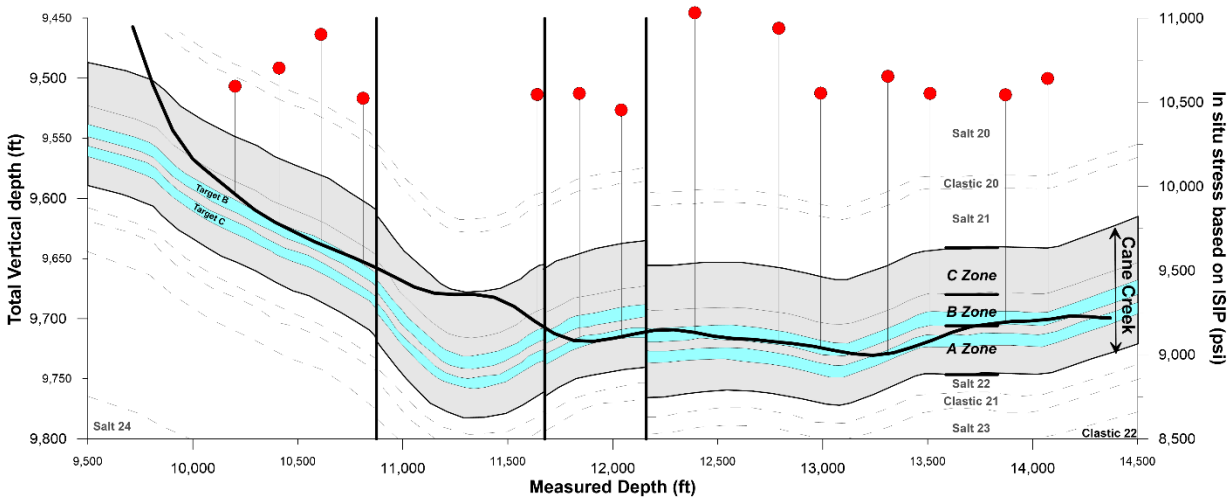

Figure 3. State 16-2 LN well placement within the Cane Creek Play. Initial Shut-In Pressure (ISIP) and related stratigraphic units are depicted by red dots and vertical lines. The Cane Creek unit's A Zone is a complex mix of dolomitic mudstone, calcareous materials, anhydrite, and siltstone, with fractures indicating high hydrocarbon potential due to rich organic content and the presence of both Type I and II kerogen. The B Zone features bioturbated siltstone-sandstone with 17% porosity, minimal anhydrite, and potential for micro- to nano-scale porosity, highlighted by its reservoir quality and identified as 'Target B' due to its high porosity and permeability. The C Zone combines both reservoir and source rock qualities with dolomitic mudstone, anhydrite, and a notable thick arkosic sandstone layer, 'Target C', showing 7 to 10% porosity and 0.197 mD permeability, alongside organic-rich mudstone with 7.9% TOC and 0.79 %Vro maturity.

Modeling Approach

The limited triggering potential of natural fractures shown by Dvory et al. (2024) and the lower production rates in well 16-2 LN due to salt obstructing production demonstrate the extent of the propagation of hydraulic fractures into the salts and the limited efficiency of hydraulic fracturing for natural fracture reactivation in the Cane Creek Unit. It is feasible that a major stimulation challenge is to increase natural fracture shearing and to create new shear fractures while constraining the hydraulic fracture propagation to the Cane Creek Unit (not extending into the salts). Recent field-scale observations, such as microseismic measurements and offset well hits, have depicted predominantly linear hydraulic fracture growth that encompasses intricate patterns like branching, twist hackles, and stepovers, as noted by (Ugueto et al., 2021; Gale et al., 2018, 2021). Here, we adopted the 'planar fracture modeling' approach to assess the potential of fracture propagation constraint (McClure and Kang, 2018; McClure et al., 2022).

The baseline simulations were based on Stage 11 field data. As indicated, this stage was slickwater and 20/40 Northern White proppant, pumped into five perforation clusters spaced over a 160-ft stage length. The calibrated baseline simulation was then modified to account for various cluster spacings and reduced fluid and proppant quantities.

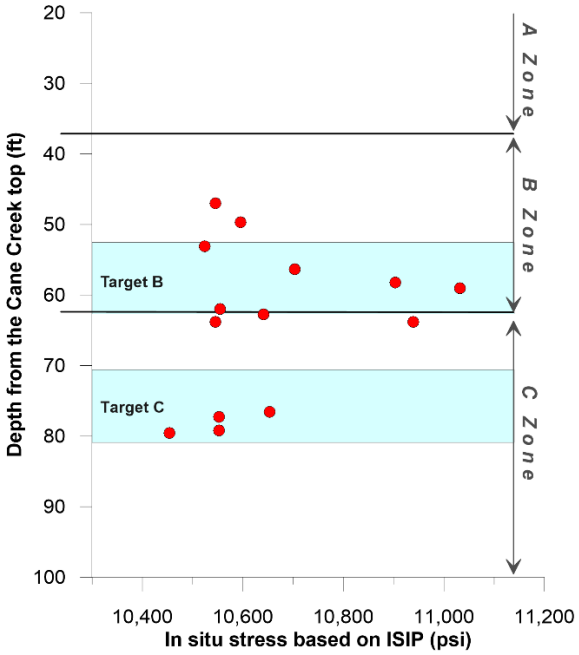

Figure 4. Stress layering profile compiled from Initial Shut-In Pressure (ISIP) measurements.

Simulation setup

In the simulations, the matrix is represented by a rectilinear grid, finely tuned perpendicular to fractures, as shown in Figure 5. An artificial ‘external fracture’ was added to the well's toe side in the model to address stress shadows from earlier stages. The viscoelastic stress relaxation method was used for initial S_{hmin} estimation, leveraging geophysical logs and the DFIT measurement for calibration to represent the variation of the minimum total horizontal principal stress with depth. This technique is based on a geomechanical model of viscoelastic stress relaxation in clay-rich rocks and predicts continuous S_{hmin} variations with depth (Gale et al., 2018, 2021).

Calibration

We performed 71 simulations, systematically varying parameters that included permeability, matrix-fracture flow, leak-off, proppant immobilization, fracture toughness, fracture strands per swarm, and wellbore friction. The 'Base' simulation was the best-fitted model through the history match procedure, indicating a robust and well-constrained match. This history match to surface treating pressure is shown in Figure 6.

One of the parameters (numerical and physical) most influential in the simulations was an unknown 'fracture strands per swarm' parameter, significantly influencing mechanical resistance to fracture propagation. The model history match illustrated in Figure 6 shows that this parameter best-fitted setting is of three strands per swarm. This result aligns with field observations from the HFTS-2 Slant Core (Gale et al., 2021). Furthermore, an inverse relationship between the strands per swarm and effective viscosity suggests that controlling fracture length through increased fracturing fluid viscosity is a viable strategy, as supported by Fu et al. (2021). The value of three fracture strands per swarm parameter also implies limited leak-off acceleration were relatively, more fluids remains in fractures at shut in, indicating a potential for secondary fracture closure in unpropped fracture strands as pressure diminishes.

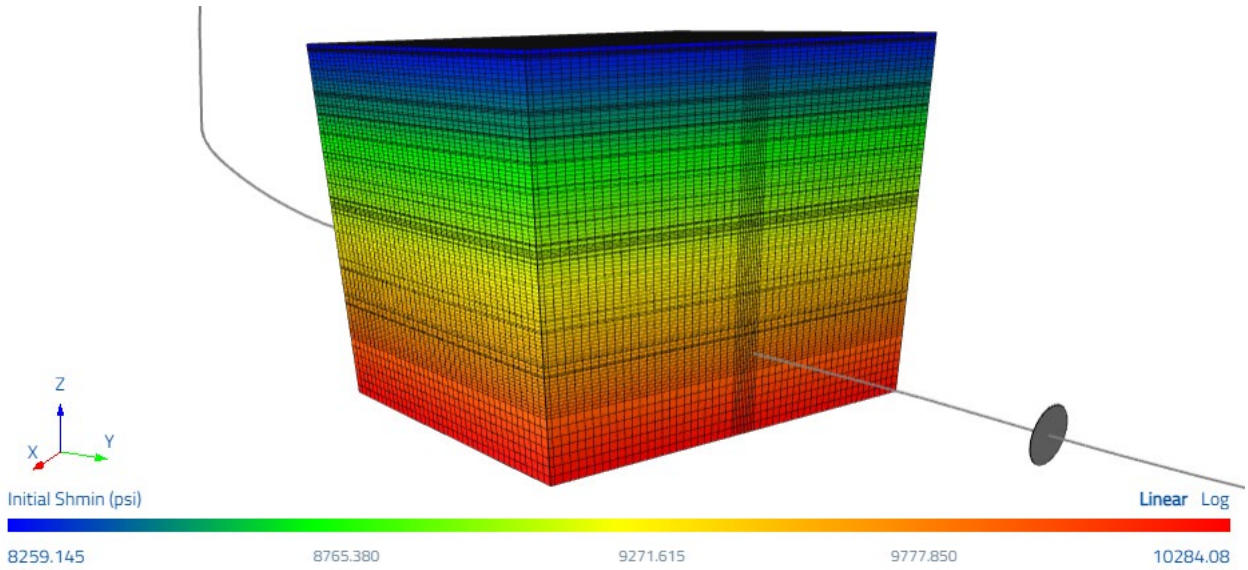

Figure 5. The simulation grid used in this study features a refined mesh perpendicular to the fractures, enhancing the accuracy of the model. The color scale represents the initial stress state. The external fracture location is marked by an oval-gray polygon. Grid dimensions: Vertical: 2,115 ft; S_{Hmax} direction: 6,000 ft; S_{hmin} direction 500 ft.

Using the model to explore cluster spacing and fluid volume per stage

From a geomechanical standpoint, the optimization of Cane Creek stimulation hinges on restricting the hydraulic fracture propagation to the Cane Creek play domain – avoiding the salts. A successful stimulation should avoid the salt and possibly triggering adjacent shearing in the pay zone. To achieve this, we tested designs that are based on tightening cluster spacing and fluid volume reduction. Tightening the spacing and reducing fluid volumes may decrease fracture length by reducing the fluid volume in each individual fracture. Another benefit is that the Cane Creek Unit would be more effectively stimulated with tighter

cluster spacing. We compared 9 designs with cluster spacing of 32 ft (base simulation), 16 ft, and 10 ft, and fluid volumes of 100%, 50%, and 25% of the original stimulation volumes (Table 2).

Table 2. Cluster spacing and fluid volume in the different stage designs. Simulation 1 represents the Stage 11 calibrated baseline simulation shown in Figure 6.

Simulation	**1**	**2**	**3**	**4**	**5**	**6**	**7**	**8**	**9**
Percentage of fluid and proppant[1] (%)	100	50	25	100	50	25	100	50	25
Length (ft)	160								
Clusters	5			10			16		
Spacing (ft)	32			16			10		

1. Percentage of fluid and proppant comparing to the volume used at the Stage 11 volumes (2,476 bbl fluids and 217,680 lb proppant)

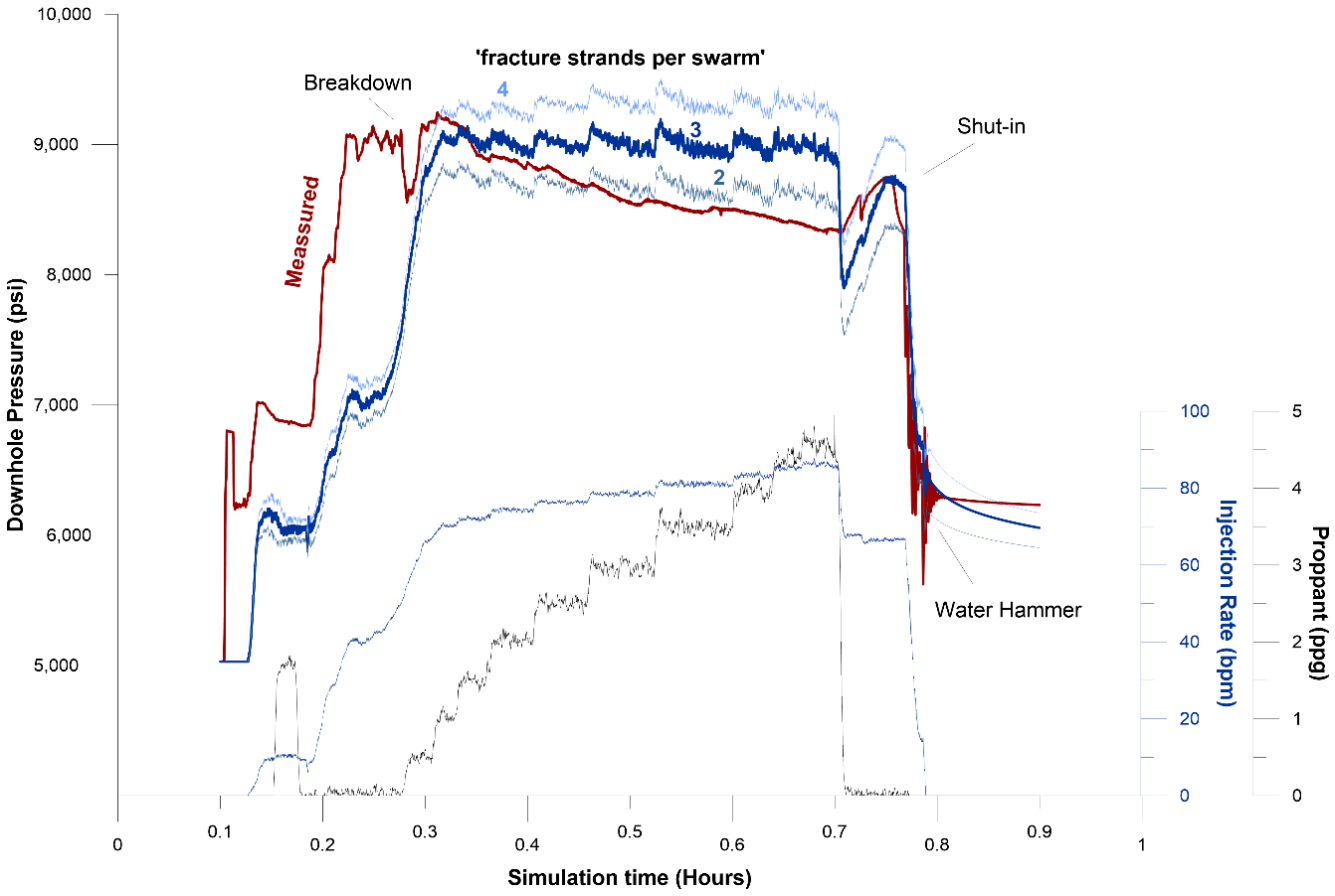

Figure 6. Graphical representation of measured pressure, injection rate, and proppant rate, alongside modeled pressures based on a 'fracture strands per swarm' range of 2 to 4.

Results and Discussion

Fracture propagations into the salt units

Figure 7 shows the predicted fracture geometry simulated in the 'Base' scenario, observed one hour after shutdown. The figure has green planes highlighting the Cane Creek Play's upper and lower limits. In this simulation, the combined effects of stress layering and the relatively low fracture toughness of the Cane Creek Play and the overlying and underlying salt layers lead to an ellipsoidal fracture geometry. This geometry results in significant propagation into the salts, extending approximately 230 feet below and 350 feet above the perforations toward sections with lower S_{hmin} values. In the Cane Creek unit, fractures are shorter in lateral length when compared to their length in the adjacent salt layers above and below. This difference is attributed to the salt's lower fracture toughness, which allows fractures to expand more laterally once they move beyond the clastic layers of the Cane Creek unit. Essentially, the physical property of the salt, being less resistant to fracturing, facilitates a broader spread of the fractures in the horizontal direction once they enter these salt units. Overall, the lateral extension of fractures within the Cane Creek layer is around 200 feet from the wellbore. As expected, the fracture nearest to the heel exhibits a substantially larger opening and higher conductivity, extending into the salt layers (Figures 7a and 7d). One hour after shutdown (or much sooner), the pressure within the fractures becomes more uniformly distributed (Figure 7b) since injection-related wall friction losses are absent. Of particular interest, the proppant distribution is inconsistent, tending to settle in distinct packets, with a considerable amount accumulating in the salts beneath the well (Figure 7e) – again as expected. The favored propagation of the fracture from the most upstream cluster results in stress shadowing, which restricts both the lateral (Figure 7f) and vertical (Figure 7c) growth of subsequent fractures. Nonetheless, the overall dimensions of all fractures become fairly uniform, indicating a balanced fracture development influenced by the interplay of geological and operational parameters.

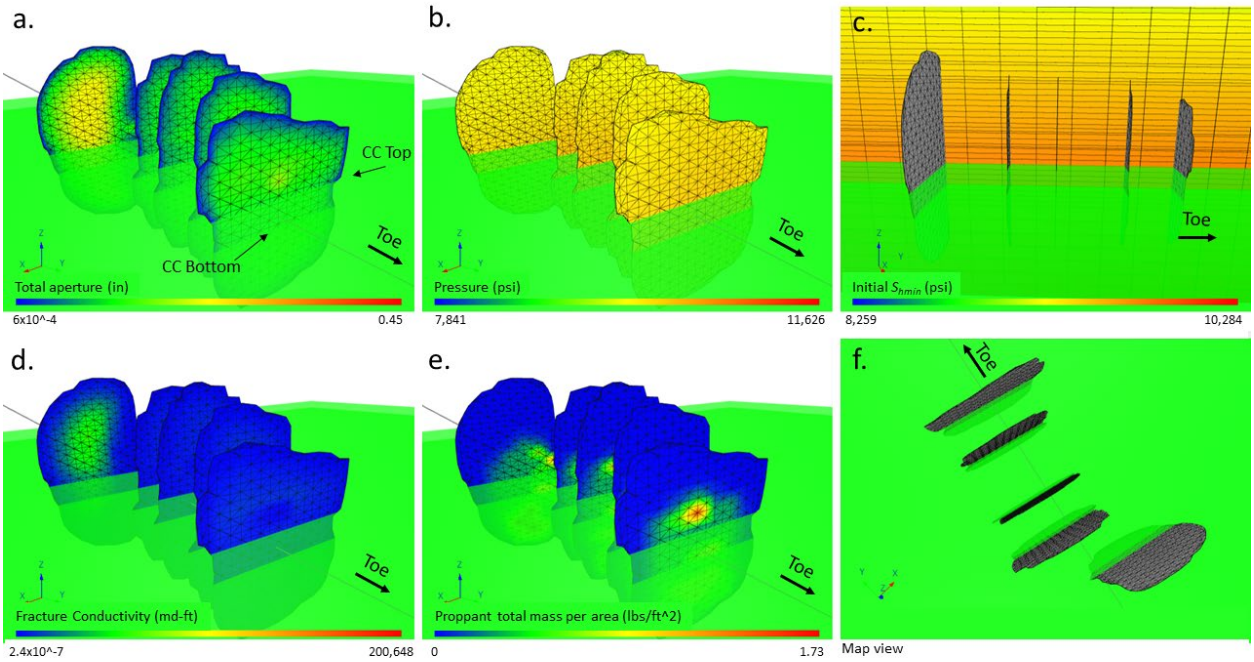

Figure 7: Visualization of fracture geometry for the 'base' simulation, captured 1-hour post-shutdown. CC is the Cane Creek unit upper and lower boundary. (a) Total aperture of fractures; (b) Pressure distribution; (c) Horizontal cross-section with initial S_{hmin} in the matrix; (d) Fracture conductivity analysis; (e) Proppant distribution patterns; and (f) Overhead (map view) of the fracture network. The green planes demarcate the upper and lower boundaries of the Cane Creek Play.

Impact of cluster spacing and fluid/proppant volume on stress shadowing and fracture geometry

Figures 8 to 15 showcase the forecasted fracture geometries, as defined by the parameters shown in Table 1. The fractures exhibit an asymmetric distribution for all cases, with the tightened cluster spacing designs highlighting the profound impact of stress shadowing. Notably, in the 10 and 16 cluster scenarios, at least one fracture either failed to initiate or did not propagate significantly from the well. This reduced spacing leads to smaller fractures in height, length, and width, effectively focusing the proppant mass distribution within the Cane Creek Play, although some proppant inevitably enters the salt layers.

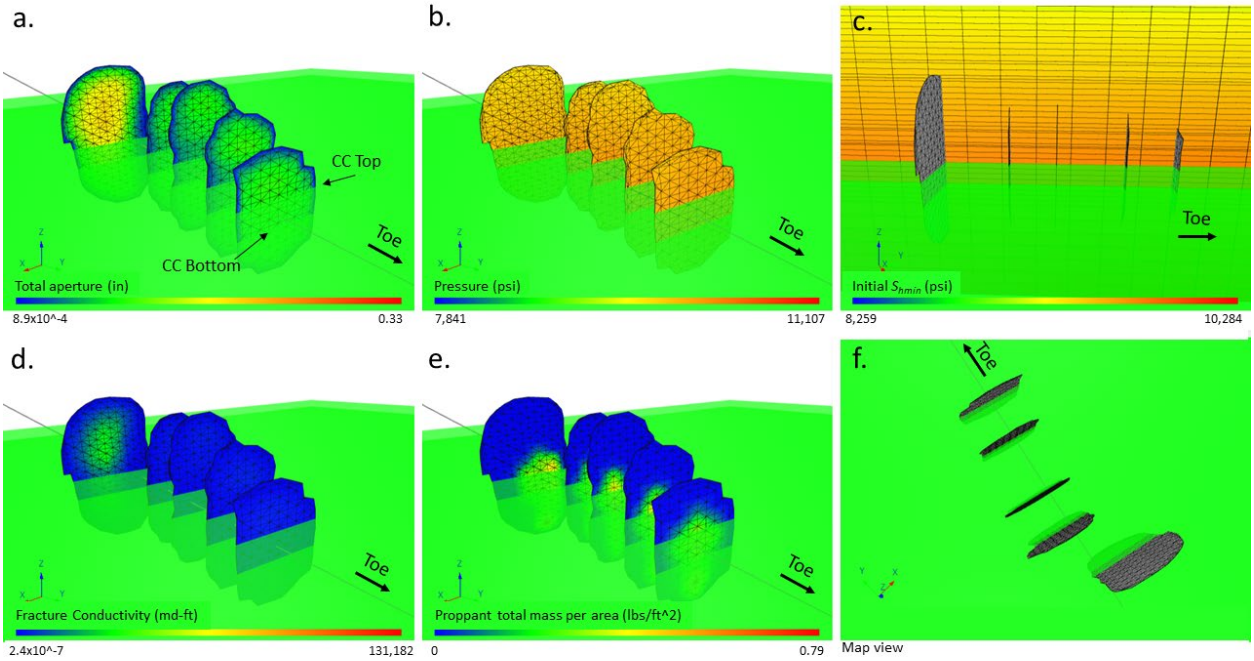

Figure 8: Visualization of fracture geometry one-hour after shutdown: Analysis of a five-cluster design with 50% reduced fluid and proppant volumes. (a) Total aperture of fractures; (b) Pressure distribution; (c) Horizontal cross-section with initial S_{hmin} in the matrix; (d) Fracture conductivity analysis; (e) Proppant distribution patterns; and (f) Overhead (map view) of the fracture network. The green planes demarcate the upper and lower boundaries of the Cane Creek Play.

A key benefit of a “tightened” spacing approach (clusters spaced more closely) is the acceleration of the near-field stress shadow response by these smaller fractures, potentially activating natural fracture shearing near the well (Dvory et al., 2024). This enhances productivity closer to the well rather than at a distance. Consistently, the fracture nearest to the heel emerges as the dominant one in terms of size, proppant distribution, and conductivity. In the Stage 11 original design (Base simulation), subsequent fractures primarily developed on the well's opposite lateral side, except for the fifth fracture (closer to the toe), which extended on both sides (seen in Figure 7f).

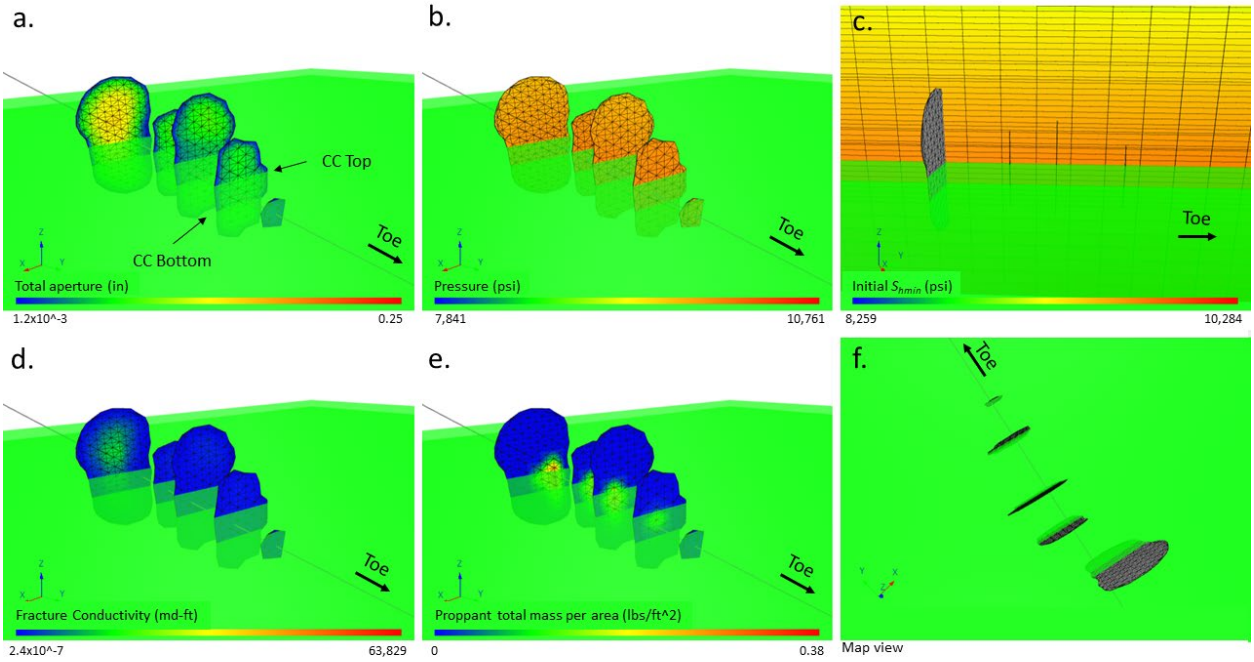

Figure 9: Visualization of fracture geometry one-hour post-shutdown: Analysis of a 5-Cluster design with 25% reduced fluid and proppant volumes. (a) Total aperture of fractures; (b) Pressure distribution; (c) Horizontal cross-section with initial S_{hmin} in the matrix; (d) Fracture conductivity analysis; (e) Proppant distribution patterns; and (f) Overhead (map view) of the fracture network. The green planes demarcate the upper and lower boundaries of the Cane Creek Play.

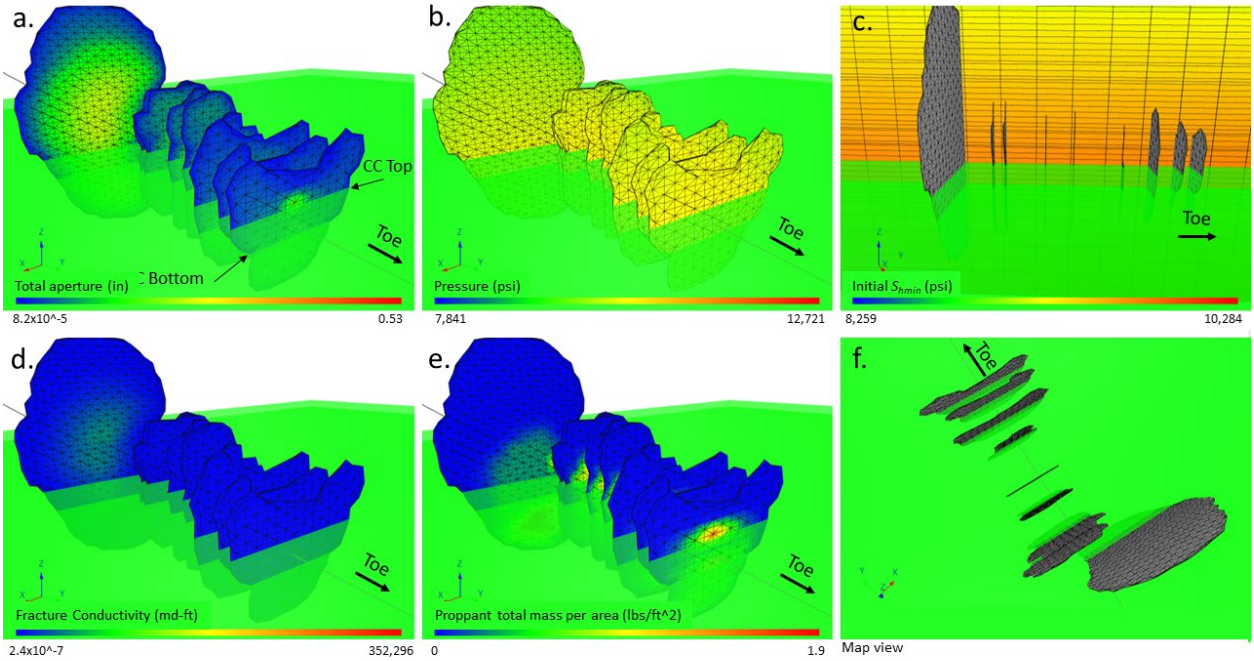

Figure 10: Visualization of fracture geometry one-hour post-shutdown: Analysis of a 10-Cluster design with stage 11 original fluid and proppant volumes. (a) Total aperture of fractures; (b) Pressure distribution; (c) Horizontal cross-section with initial S_{hmin} in the matrix; (d) Fracture conductivity analysis; (e) Proppant distribution patterns; and (f) Overhead (map view) of the fracture network. The green planes demarcate the upper and lower boundaries of the Cane Creek Play.

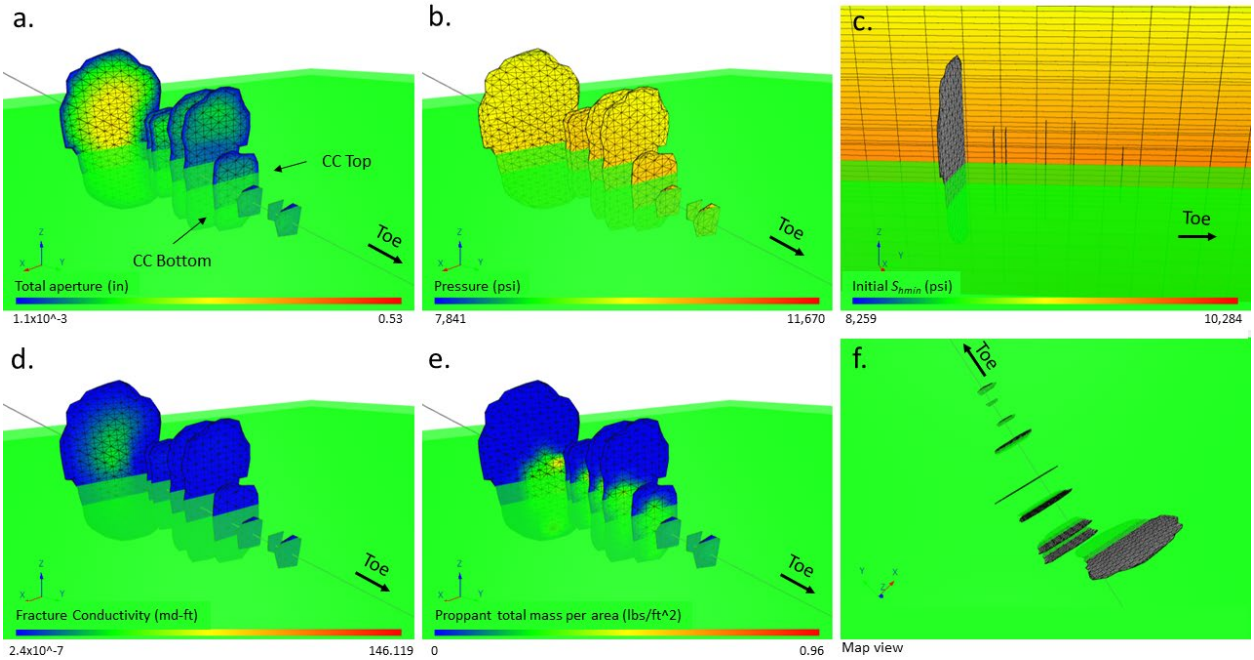

Figure 11: Visualization of fracture geometry one-hour post-shutdown: Analysis of a 10-Cluster design with 50% reduced fluid and proppant volumes. (a) Total aperture of fractures; (b) Pressure distribution; (c) Horizontal cross-section with initial S_{hmin} in the matrix; (d) Fracture conductivity analysis; (e) Proppant distribution patterns; and (f) Overhead (map view) of the fracture network. The green planes demarcate the upper and lower boundaries of the Cane Creek Play.

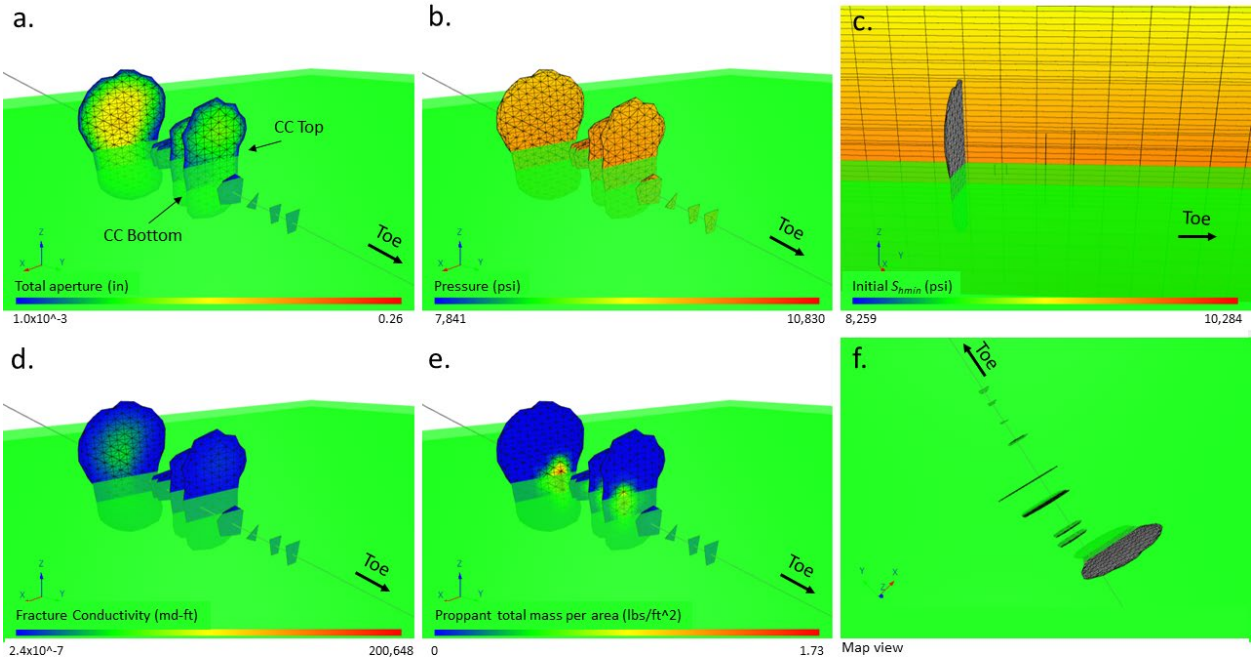

Figure 12: Visualization of fracture geometry one-hour post-shutdown: Analysis of a 10-Cluster design with 25% reduced fluid and proppant volumes. (a) Total aperture of fractures; (b) Pressure distribution; (c) Horizontal cross-section with initial S_{hmin} in the matrix; (d) Fracture conductivity analysis; (e) Proppant distribution patterns; and (f) Overhead (map view) of the fracture network. The green planes demarcate the upper and lower boundaries of the Cane Creek Play.

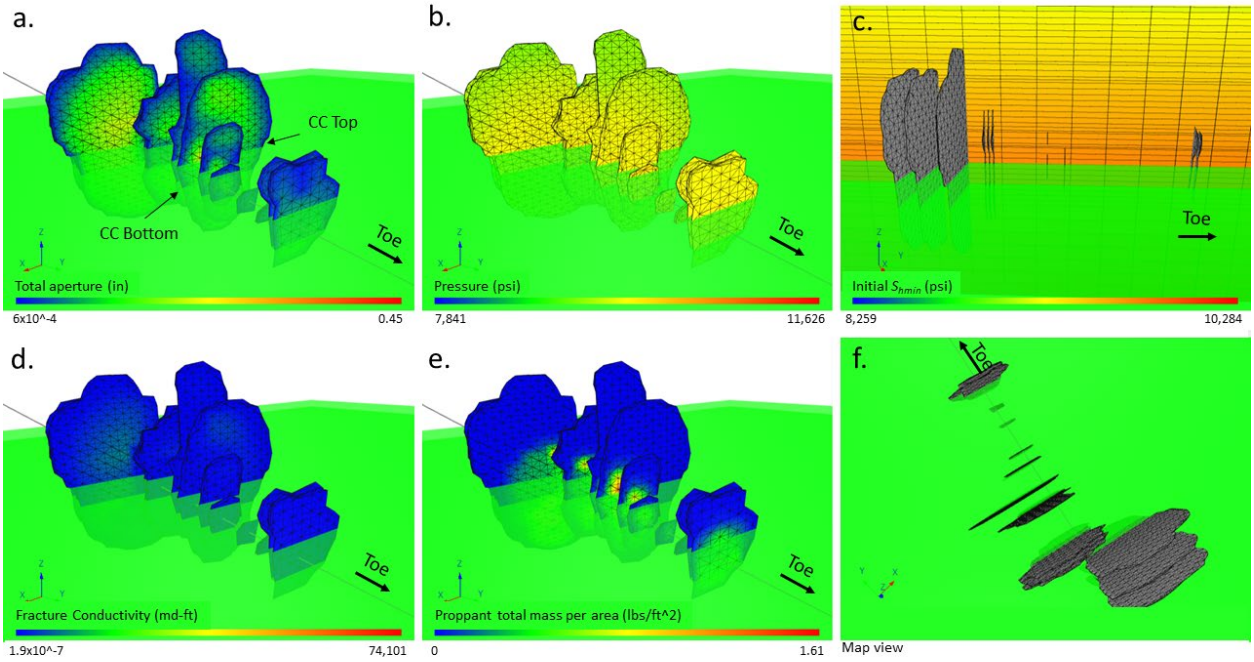

Figure 13: Visualization of fracture geometry one-hour post-shutdown: Analysis of a 16-Cluster design with stage 11 original fluid and proppant volumes. (a) Total aperture of fractures; (b) Pressure distribution; (c) Horizontal cross-section with initial S_{hmin} in the matrix; (d) Fracture conductivity analysis; (e) Proppant distribution patterns; and (f) Overhead (map view) of the fracture network. The green planes demarcate the upper and lower boundaries of the Cane Creek Play.

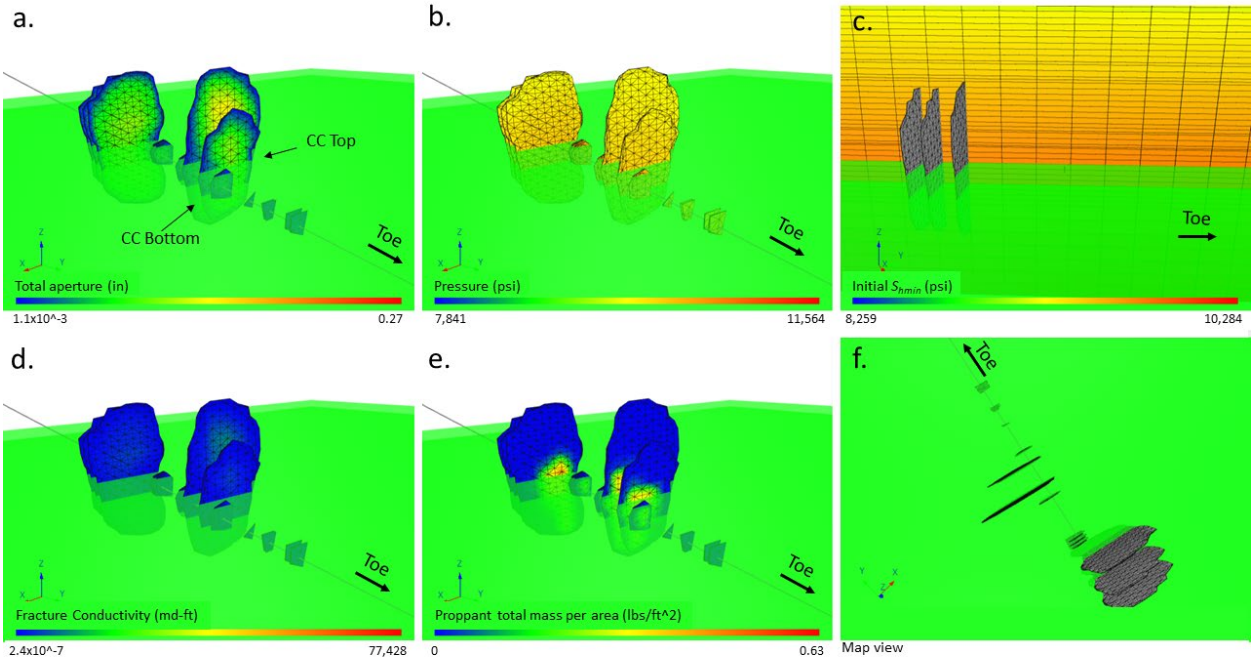

Figure 14: Visualization of fracture geometry one-hour post-shutdown: Analysis of a 16-Cluster design with 50% reduced fluid and proppant volumes. (a) Total aperture of fractures; (b) Pressure distribution; (c) Horizontal cross-section with initial S_{hmin} in the matrix; (d) Fracture conductivity analysis; (e) Proppant distribution patterns; and (f) Overhead (map view) of the fracture network. The green planes demarcate the upper and lower boundaries of the Cane Creek Play.

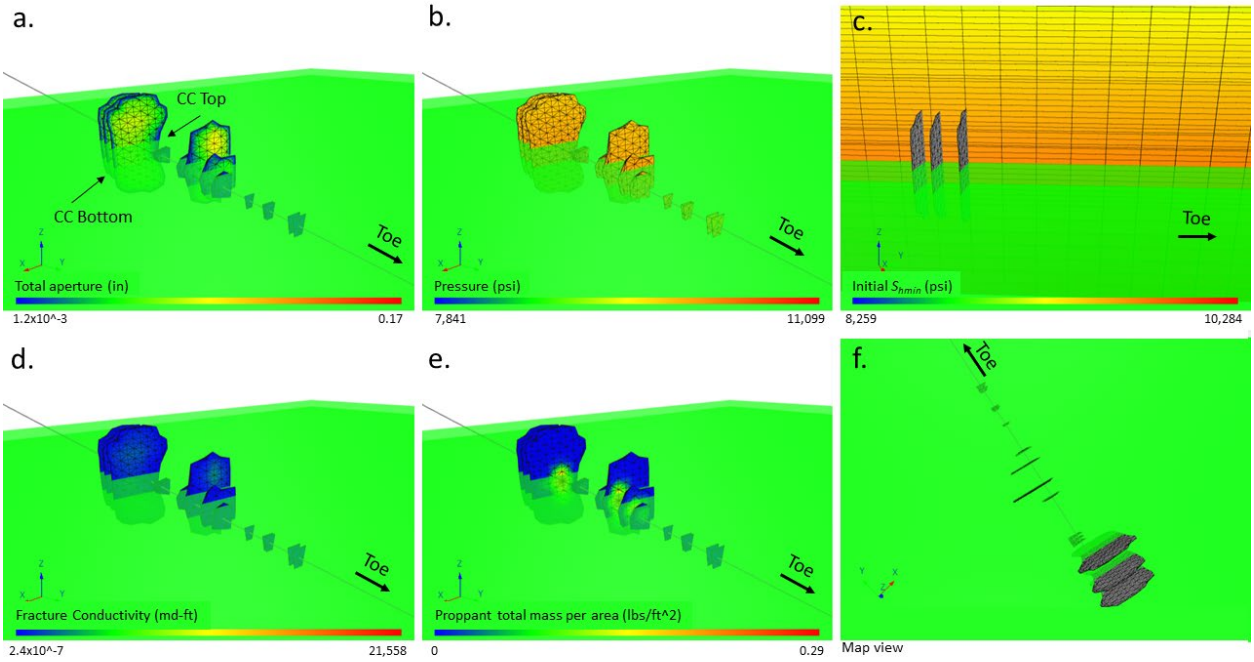

Figure 15: Visualization of fracture geometry one-hour post-shutdown: Analysis of a 16-cluster design with 25% reduced fluid and proppant volumes. (a) Total aperture of fractures; (b) Pressure distribution; (c) Horizontal cross-section with initial S_{hmin} in the matrix; (d) Fracture conductivity analysis; (e) Proppant distribution patterns; and (f) Overhead (map view) of the fracture network. The green planes demarcate the upper and lower boundaries of the Cane Creek Play.

Reducing the fluid volume and proppant mass in the five-cluster design by 50% and 25% yielded a similar spatial distribution of the fracture's geometry but with reduced intensity. In other words, the stress shadow influences how fractures spread and their shape and the extent and pattern of fracture development are constrained by the amount of fluid injected. An indicator of the most upstream fracture's stress shadow extent is suggested by the slightly heightened third fracture. The fifth fracture in the 25% reduction scenario barely extends into the salts, as shown in Figure 9. In the 10-cluster design, the initial fracture is markedly larger than the others, with the last three fractures appearing less affected by the "first" fracture's stress shadow effect (Figure 10f). The fourth and fifth fractures in the 50% and 25% reduction designs are overall larger than adjacent fractures, indicating the boundary of the first fracture's stress shadow distribution (Figures 11 and 12). The 16-cluster design with base case fluid and proppant volumes displays three larger fractures near the heel, five intermediate fractures in the middle of the stimulated section, and farther, only the last two begin to increase in height (Figure 13). In the 50% and 25% reduction designs the fracture height at the stage's middle section is relatively higher than the adjusted fractures. The relatively high fraction in the middle of the stimulated section is also seen at the 5 and 10-cluster with the reduced volume and mass designs. (Figures 14 and 15), reinforcing the observed limited stress shadow effect trend as the injected volume is reduced.

The simulations highlight potential operational considerations. With the baseline injection volume (consistent with a typical stage pumped in a representative offset well), the overall fracture surface area within the play increased by 38% in the 10-cluster design and 60% in the 16-cluster design, as shown in Figure 16. Reducing fluid and proppant volumes moderates this increase, particularly in the 16-cluster design, demonstrating a heightened sensitivity to volume reduction. This emphasizes the influence of injection volumes in tight spacing designs, especially regarding near-field stimulation effects.

Figure 17 compares the fracture surface within the Cane Creek unit and the overall fracture surface area for each of the simulations described in Table 2, allowing for an assessment of each design's appropriateness. When considering injection volume, the base case volume coupled with different cluster designs indicates

that the highest fracture surface area within the Cane Creek reservoir is for a 16-cluster design with the original Stage 11 injection volume. However, a significant portion, at least 55%, of the total fracture surface extends into the salt layers.

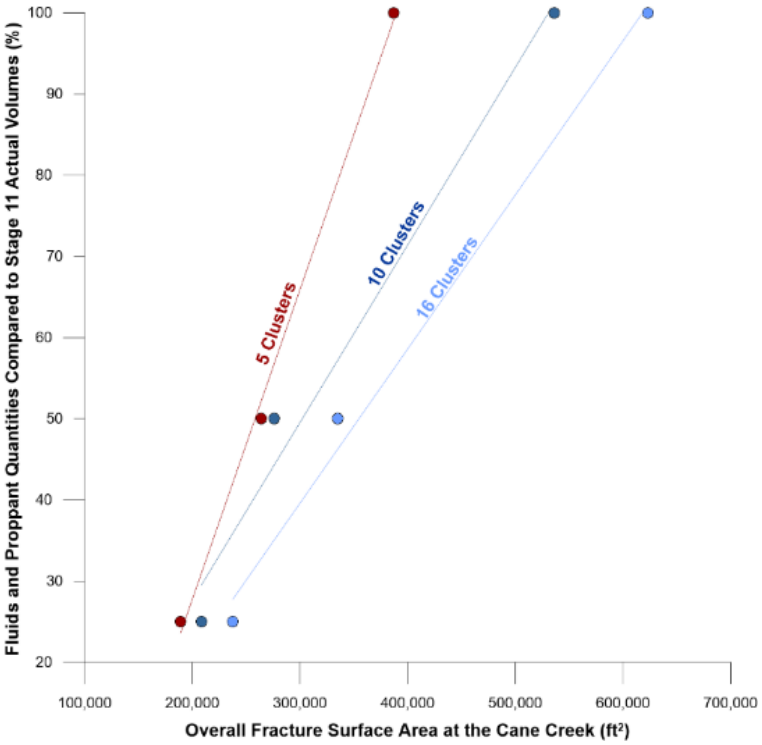

Figure 16. Correlation of overall fracture surface area with fluid volume and proppant mass variations in the Cane Creek Play

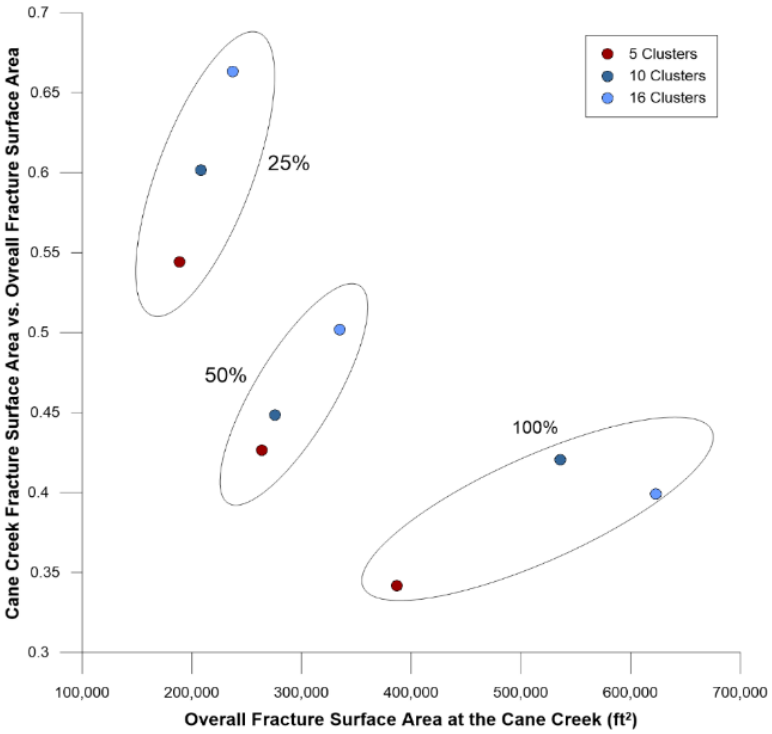

Figure 17. Impact of injection volumes on relative fracture surface area within the Cane Creek Play.

In contrast to the 16-cluster design with baseline injection volume, the 16-cluster design with a 25% reduction in injection volume leads to a more balanced ratio between the Cane Creek surface area and the salts, with less than 33% of the fracture area extending into the salts. In this scenario, the fracture surface area within the Cane Creek Unit is about 60% of that in the original design. The 60% less surface area in the Cane Creek reduces production by 40%. Still, the exposure to the salt is reduced to 13% of the original stimulation, suggesting this approach is a viable option. This reduced volume design could lead to better production efficiency and lower operational costs due to decreased halite precipitation in fractures and tubulars, offering a potentially more cost-effective and productive operational strategy.

Conclusions

This evaluation of the Cane Creek Play in the Paradox Formation has provided insights into optimizing hydraulic fracturing strategies in this challenging yet promising tight oil play. The primary focus has been on controlling fracture propagation within the oil-bearing zones and minimizing extension into adjacent salt formations, which are known to cause operational difficulties and reduced production.

Our findings emphasize the critical role of fracture toughness and stress layering in determining fracture propagation patterns. In other words, there is no real impediment to pseudoradial fracture growth and significant contact with the neighboring salts. The relatively lower fracture toughness of both the clastics and the salt layers in the Paradox formation necessitates careful design of fracturing operations to limit fracture extension and maintain fractures within the productive zones. Additionally, adjusting cluster spacing and fluid volume emerged as effective strategies for managing fracture propagation. Tighter cluster spacing and reduced fluid volumes led to more efficient stimulation within the Cane Creek Play, with a significant reduction in fracture extension into non-target salt layers. Specifically, our analysis of fracture surface areas within the Cane Creek against various simulation designs shows that the extended cluster design achieves the highest fracture surface area in the target formation but risks extensive fracture extension into salt layers, compromising operational efficiency. Conversely, reducing the injection volume for the same cluster design significantly mitigates salt layer exposure while maintaining a substantial portion of the productive fracture area within the pay zone. This approach not only lowers the risk of halite precipitation, which can hamper production but also suggests a more cost-effective strategy by balancing productive surface area with operational risks. Ultimately, the findings advocate for a tailored approach in hydraulic fracturing design, emphasizing the need to carefully consider both geological characteristics and operational parameters to optimize production outcomes and reduce costs.

Acknowledgments

This study was funded by the DOE project: Improving Production in the Emerging Paradox Oil Play DEFE0031775. We thank Mark McClure for his useful comments and the ResFrac academic.

References

Cooper, S., and J. Lorenz, 2022, Assessment of Natural Fractures in Core from the State 16-2 Well, Cane Creek Fm, Utah.

Dontsov, E. V., and R. Suarez-Rivera, 2020, Propagation of multiple hydraulic fractures in different regimes: International Journal of Rock Mechanics and Mining Sciences, v. 128, p. 104270, doi:10.1016/j.ijrmms.2020.104270.

Dvory, N. Z., J. D. McLennan, and B. J. McPherson, 2024, Optimizing Hydraulic Fracturing in the Paradox Formation: A Geomechanical Study of the Cane Creek Play: American Rock Mechanics Association, v. ARMA 24–1158.

Fu, P., J. Huang, R. R. Settgast, J. P. Morris, and F. J. Ryerson, 2019, Apparent Toughness Anisotropy Induced by "Roughness" of In-Situ Stress: A Mechanism That Hinders Vertical Growth of Hydraulic Fractures and Its Simplified Modeling: SPE Journal, v. 24, no. 05, p. 2148–2162, doi:10.2118/194359-PA.

Fu, W., J. P. Morris, P. Fu, J. Huang, C. S. Sherman, R. R. Settgast, and F. J. Ryerson, 2021, Developing Upscaling Approach for Swarming Hydraulic Fractures Observed at Hydraulic Fracturing Test Site through Multiscale Simulations: SPE Journal, v. 26, no. 05, p. 2670–2684, doi:10.2118/199689-PA.

Gale, J. F. W., S. J. Elliott, and S. E. Laubach, 2018, Hydraulic Fractures in Core From Stimulated Reservoirs: Core Fracture Description of HFTS Slant Core, Midland Basin, West Texas, *in* Proceedings of the 6th Unconventional Resources Technology Conference, Houston, Texas, USA: American Association of Petroleum Geologists, doi:10.15530/urtec-2018-2902624.

Gale, J. F. W., Elliott, Rysak, C. L. Ginn, N. Zhang, R. D. Myers, and S. E. Laubach, 2021, Fracture Description of the HFTS-2 Slant Core, Delaware Basin, West Texas, *in* Proceedings of the 9th Unconventional Resources Technology Conference, Houston, Texas, USA: American Association of Petroleum Geologists, doi:10.15530/urtec-2021-5175.

Jagniecki, E., R. Gall, T. Wiseman, and M. Vanden Berg, 2019, Geologic Characterization of the Northern Cane Creek Shale Play, Paradox Basin, Utah.

Li, C., Yaoqing Hu, T. Meng, C. Zhang, R. Gao, P. Jin, and Yuefei Hu, 2020, Mode-I fracture toughness and mechanisms of Salt-Rock gypsum interlayers under real-time high-temperature conditions: Engineering Fracture Mechanics, v. 240, p. 107357, doi:10.1016/j.engfracmech.2020.107357.

McClure, M., and C. Kang, 2018, ResFrac Technical Writeup.

McClure, M., M. Picone, G. Fowler, D. Ratcliff, C. Kang, S. Medam, and J. Frantz, 2020, Nuances and Frequently Asked Questions in Field-Scale Hydraulic Fracture Modeling: no. 1, p. 1–19, doi:10.2118/199726-ms.

Meng, T., Y. Hu, R. Fang, J. Kok, Q. Fu, and G. Feng, 2015, Study of fracture toughness and weakening mechanisms in gypsum interlayers in corrosive environments: Journal of Natural Gas Science and Engineering, v. 26, p. 356–366, doi:10.1016/j.jngse.2015.06.027.

Simonson, R., 1978, Containment of Massive Hydraulic Fractures: SOCIETY OF PETROLEUM ENGINEERS JOURNAL.

Singh, A., M. Zoback, and M. McClure, 2020, Optimization of Multi-Stage Hydraulic Fracturing in Unconventional Reservoirs in the Context of Stress Variations with Depth, *in* Day 3 Wed, October 28, 2020, Virtual: SPE, p. D031S025R007, doi:10.2118/201739-MS.

Ugueto, G. A., M. Wojtaszek, P. T. Huckabee, A. A. Savitski, A. Guzik, G. Jin, J. A. Chavarria, and K. Haustveit, 2021, An Integrated View of Hydraulic Induced Fracture Geometry in Hydraulic Fracture Test Site 2, *in* Proceedings of the 9th Unconventional Resources Technology Conference, Houston, Texas, USA: American Association of Petroleum Geologists, doi:10.15530/urtec-2021-5396.

Wang, Z., X. Liang, X. Guangwu, T. Meng, and J. Zhang, 2022, Creep Fracture Characteristics and the Constitutive Model of Salt Rock under a Coupled Thermo-Mechanical Environment: Mathematical Problems in Engineering, v. 2022, p. 1–14, doi:10.1155/2022/4926917.